PO Box 2345, Beijing 100023, China
www.wjgnet.com
wjg@wjgnet.com

ELSEVIER

World J Gastroenterol 2005;11(35):5506-5511
World Journal of Gastroenterology ISSN 1007-9327

• *BASIC RESEARCH* •

MR diffusion-weighed imaging of rabbit liver

You-Hong Yuan, En-Hua Xiao, Zhong He, Jun Xiang, Ke-Li Tang, Rong-Hua Yan, Ke Jin, Zi-Wen Peng

You-Hong Yuan, En-Hua Xiao, Zhong He, Jun Xiang, Ke-Li Tang, Rong-Hua Yan, Ke Jin, Zi-Wen Peng, Department of Radiology, the Second Xiangya Hospital, Central South University, Changsha 410011, Hunan Province, China
Supported by the National Natural Science Foundation of China, No. 30070235, 30470508; Science Foundation of Hunan Province, No. 202064, 04-SK-306-2
Correspondence to: Dr. En-Hua Xiao, Department of Radiology, the Second Xiangya Hospital, Central South University, Changsha 410011, Hunan Province, China. xiaogdk@sohu.com
Telephone: +86-731-5550355 Fax: +86-731-4510190
Received: 2004-07-26 Accepted: 2004-12-29

Abstract

AIM: To study the techniques of MR diffusion-weighed imaging (DWI) for normal rabbit liver.

METHODS: After 15 normal New Zealand white rabbits and one New Zealand white rabbit implanted with VX-2 tumor were anesthetized with 3% soluble pentobarbitone, DWI was performed respectively for different *b* values, repetition times (TR) or thicknesses, when other parameters were the same and magnetic resonance imaging (MRI) was performed respectively, or with different field of views (FOV) or coil when other parameters were the same. The distinction between groups was analyzed by SPSS10.0 with apparent diffusion coefficient (ADC), quality index (QI) or signal-noise ratio (SNR).

RESULTS: As *b* value increased, liver ADC, QI and SNR of DWI became smaller and simultaneously (F = 292.87, 156.1, 88.23, P<0.01). QI of DWI was high, when *b* value was 10, 50 or 100 respectively, but the distinction between them was insignificant; when *b* value was 800, QI and SNR of DWI were low. QI and SNR of DWI had no significant difference between TR = 4 000, 6 000 and 8 000. QI of DWI with 2 mm thickness was bigger than that with 5 mm thickness (t = 3.04, P<0.01), but SNR of DWI with 2 mm thickness was significantly smaller (t = -17.86, P<0.01). SNR of MRI with knee joint coil was obviously bigger than that with cranium coil [t = -5.77 (T1WI) or -4.02 (T2WI), P<0.01], but QI of MRI was smaller on the contrary [t = 7.10 (T1WI) or 3.97 (T2WI), P<0.01]. When FOV was enlarged gradually, SNR of MRI increased [F = 85.81 (T1WI) or 221.96 (T2WI), P<0.01], but QI firstly increased, then decreased [F = 68.67 (T1WI) or 69.46 (T2WI), P<0.01] and QI of MRI was the biggest when FOV was 20 cm×15 cm.

CONCLUSION: The scanning technique is very important in DWI of rabbit liver and the overall quality of DWI with *b* (100 s/mm^2), thickness (2 mm), cranium coils and FOV (20 cm×15 cm) was best in our study, when other parameters were the same.

Key words: Liver; Rabbits; Magnetic resonance imaging; Diffusion-weighted imaging; Technology

Yuan YH, Xiao EH, He Z, Xiang J, Tang KL, Yan RH, Jin K, Peng ZW. MR diffusion-weighed imaging of rabbit liver. *World J Gastroenterol* 2005; 11(35): 5506-5511
http://www.wjgnet.com/1007-9327/11/5506.asp

INTRODUCTION

Hepatocellular carcinoma (HCC) is one of the most frequent malignant tumors[1]. Many researches on its computed tomography (CT)[2-6], ultrasonography (US)[4-8] and digital subtraction angiography (DSA)[7-9] have been performed in recent years and they have demonstrated their significant values in diagnosis or prognosis of HCC.

However, the application of MRI[10-14], especially diffusion-weighted imaging (DWI)[14-16], in diagnosing hepatic tumors and evaluating its progression is much less than that of CT and US. With the development of software and the scanning technology of MRI, common MRI, including T1WI, T2WI of the axial, the coronal or the sagittal and magnetic resonance cholangiopancreatography (MRCP), has been used widely in diagnosing and evaluating progression of hepatic tumors in recent years.

Diffusion is caused by random water molecular motion. The amount of diffusion is determined by diffusion coefficient. However, because the measurement of the diffusion coefficient (DC) *in vivo* may be affected by many factors, such as temperature, blood perfusion, magnetic susceptibility in the tissue, or other kinds of motion, more of apparent diffusion coefficient (ADC) rather than DC is used clinically[17-19]. DWI was initially used to evaluate early ischemic stages of the brain and its value has been accepted in recent years all over the world. Meanwhile, several research groups have concluded that DWI has great potential for understanding normal and pathological brain function[20-22]. But only a few researches, including that of Inoha *et al.*[23,24], and Geschwind *et al.*[14], on the value of DWI in diagnosing or evaluating the progression of hepatic lesions, especially VX-2 tumor of rabbit, have been reported.

The rabbit VX-2 tumor, today, is seen as the valued animal modality of HCC in researching its imaging characteristics, because most experiments have demonstrated that the blood supply of VX-2 tumor is similar to that of HCC and VX-2 tumor is implanted easily and grows quickly so that

the diameter of the tumor can reach 2 cm or more, 3 wk after implantation and it is able to transfer or metastasize to the liver, the lump, mediastina, etc. in the early stage, and VX-2 tumor animal models have been applied increasingly in the study of HCC[10-13,24]. Thus, it is important to study the characteristics of rabbit liver MR DWI. Geschwind *et al*.[14], have performed researches on the value of DWI in assessing VX-2 tumor cell apoptosis and histologic analysis after transcatheter arterial chemoembolization (TACE). However, the study on the characteristics of rabbit liver VX-2 tumor MR DWI has not been reported. The main reason is its poor quality of imaging which greatly limits its use in diagnosing or evaluating the progression of tumors[14-17].

The purpose of our experiment is to study the techniques of MR DWI of normal rabbit liver in order to improve its image quality and to prepare for the study of MR DWI of rabbit liver VX-2 tumor, which is an important part of the HCC study on MR DWI after TACE.

MATERIALS AND METHODS

Experimental animals

The animal studies were performed under the supervision of a veterinarian and were completely compliant with the National Institutes of Health (NIH) guidelines for the use of laboratory animals. All animals were provided by the Animal Department of the Second Xiangya Hospital and all protocols were approved by the Animal Use and Care Committee of the hospital.

Of 15 New Zealand normal white rabbits, seven were male rabbits and eight were female, their weights ranging from 1.5 kg to 2.0 kg and their ages ranging from 5 mo to 6 mo. One New Zealand white rabbit was transplanted with VX-2 tumor for 21 d, and four rabbits were for pre-experiment. All New Zealand white rabbits were healthy.

Magnetic resonance imaging protocol

After animals were anesthetized, by injecting 3% soluble pentobarbitone into auricular vein at a dose of 1 mL/kg or different dose based on different animal status in order to make sure that the breath of animals was slowest, other than for the dead ones, and stable, T1WI, T2WI or DWI was performed on a 1.5-Tesla Signa Twinspeed MR scanner (General Electron Medical Systems, USA). Our experiment was divided into seven steps.

Firstly, to clearly observe the effect of animal breathing on MRI quality and choose the most suitable dose of anesthesia, T1WI and T2WI were obtained repeatedly in pre-experiment after four rabbits (excluding 15 rabbits in formal experiment) were anesthetized with different dosage, from low to high, of 3% soluble pentobarbitone injected into auricular vein. Then we compared the quality of images with that of the images after the rabbits died from an overdose of anesthesia. From this, we concluded that the quality of the images was the best, when breathing of animals was slow and stable and this dose was the most suitable anesthetic dosage. Secondly, T1WI and T2WI of 15 rabbits were obtained respectively with the cranium coil and the knee joint coil, and the other similar parameters included fast reverse fast spin echo (FRFSE) series, T1WI [(TR) 400 ms/echo time (TE) 12.3 ms], T2WI (TR3000/TE80 ms), FOV 20 cm×15 cm, NEX 4, thickness of the layer 5 mm, spacing 0 mm, matrix 256×192 (T1WI) and 320×256 (T2WI). Thirdly, different FOVs included 24 cm×24 cm, 20 cm×15 cm, 16 cm×12 cm, while the other parameters were similar to those in step two; T1WI and T2WI of 15 rabbits were carried out respectively. Fourthly, DWIs of 15 rabbits were acquired respectively for different *b* values including 10, 50, 100, 300, 800 s/ mm^2 while other parameters remained the same (Table 1). Fifthly, DWIs of 15 rabbits were performed respectively with different TR values including 4 000, 6 000, and 8 000, while the other parameters remained the same (Table 1). Sixthly, DWIs of 15 rabbits were obtained respectively for different layer thicknesses including 2 and 5 mm, while other parameters remained the same (Table 1). Finally, DWI of VX-2 tumor rabbit was performed for a *b* value of 100 or 300 s/mm^2, TR 6 000, and a 2-mm thick cranium coil.

Data analysis

Based on the ADC value of the region of interest (ROI), QI and SNR, the distinction between different scanning parameter groups was respectively evaluated quantitatively. Of them, the ADC and SNR values were obtained through GE working station.

ADC values of 15 normal rabbit liver parenchyma were obtained by getting the ADC average value from five different ROIs at the central layer of the liver, of which each area was 50 mm^2, which was measured five times, with the help of the relative functional software in GE working station.

QI value was an image marker, which was obtained by combining SNR, the artifact and the liver anatomy manifestation of the image with the same weight after they were quantified respectively with five levels, which could reflect the image

Table 1 The parameters of normal rabbit MR DWI

Series	*b*	TR	TE	FOV	NEX	Thickness	Spacing	Matrix	Coils
SE-EPI	10	6 000	45	20×15	8	2	0.5	128×128	Cranium
SE-EPI	50	6 000	45	20×15	8	2	0.5	128×128	Cranium
SE-EPI	100	6 000	45	20×15	8	2	0.5	128×128	Cranium
SE-EPI	300	6 000	45	20×15	8	2	0.5	128×128	Cranium
SE-EPI	800	6 000	45	20×15	8	2	0.5	128×128	Cranium
SE-EPI	100	4 000	45	20×15	8	2	0.5	128×128	Cranium
SE-EPI	100	6 000	45	20×15	8	2	0.5	128×128	Cranium
SE-EPI	100	8 000	45	20×15	8	2	0.5	128×128	Cranium

SE-EPI: spin echo echo planar imaging.

quality collegiately. SNR is the contrast of SH to SD. SH was the average signal of the hepatic parenchyma from the average value of five different ROIs, each area of which was 50 mm^2 excluding biliary ducts and blood vessels. SD is standard deviation of background signal intensity in the direction of the phase coding. It was obtained by calculating the average value of five ROIs which were not only in front of the abdominal wall but in the field of the scanning as well. The values of "SNR<5", "5<SNR<10", "10<SNR <20", "20<SNR<30", "30<SNR<50" and "SNR>50" are thought of as 0, 1, 2, 3, 4 and 5 scores respectively. As far as the artifact of the images is concerned, when the artifact was the highest and the images could not be used for diagnosis, we considered it as 1 score and when the artifact was very high and it affected diagnosis seriously, we considered it as 2 scores. When the artifact of the images was general and it had some effects on manifestation and diagnosis of the lesions, we regarded it as 3 scores and when the artifact was not high and it did not affect diagnosis seriously, we regarded it as 4 scores. Then, when the artifact was little or none, we regarded it as 5 scores. As for the liver anatomy manifestation of the images, 1 score represented the poorest quality of the images which could not display, at all, the border of the organ or the intrahepatic vessels and 3 scores indicated the average quality of the images which could display the border of most organs, comparatively display the major intrahepatic vessels and vaguely display the border of stomach and bowel and, then, 5 scores showed the highest quality of the images which could distinctly display the border of most organs, clearly display the intrahepatic microvessels and that of the border of the stomach and bowel. When the quality of the images was between 1 and 3 scores, we regarded it as 2 scores and, when the quality of the images was between that of 3 scores and 5 scores, we regarded it as 4 scores.

All MR images were retrospectively analyzed by three experienced radiologists and evaluation of the images artifact and liver anatomy manifestations were obtained by average value statistical analysis, based on the above criteria.

The statistical significance was calculated using SPSS10.0 with analysis of variance (ANOVA) of the randomized block design or paired *t*-test.

RESULTS

Considering only the increase in *b* value and no other parameter, the mean ADC value of hepatic parenchyma was decreased and, at the same time, QI also decreased (Table 2). The distinction of ADC among *b* values of 100 and that of 10, 50, 300 or 800 was significant, respectively (Tukey HSD, $P<0.01$). The distinction of QI among groups of *b* values 10, 50 and 100 s/mm^2 was insignificant, and those among *b* values 100, 300 or 800 was significant (Tukey HSD, $P<0.01$), and was significant between groups of *b* values of 800 and 300 (Tukey HSD, $P<0.01$). With *b* value increase, SNR became smaller and, when *b* value was 800, SNR was no more than 10 (Table 2, Figures 1 and 2). The distinction of SNR between *b* values 100, 10, 300 or 800 was significant (Tukey HSD, $P<0.01$) and that between *b* values 100 and 50 was not significant.

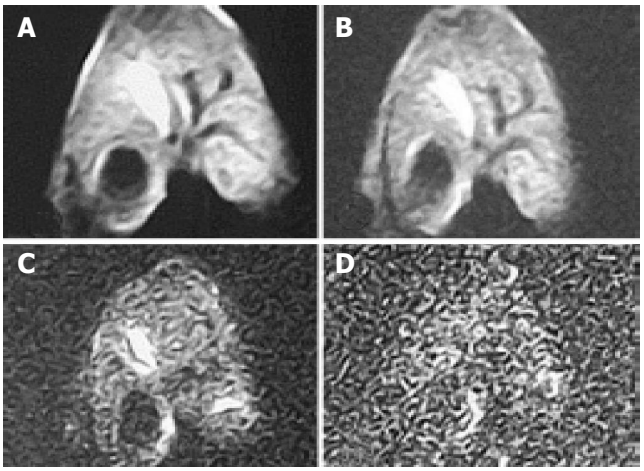

Figure 1 With *b* value, thickness, TR value, scanning coil and NEX were different, ADC value, the ability of liver anatomy manifestation or differentiation and SNR of rabbit liver on MR DWI were also different. b value were respectively 10,100, 300 and 800 s/mm^2 of the image (**A**), (**B**), (**C**) and (**D**). ADC value, SNR and the liver anatomy manifestation of the images became lower and lower with increasing b value. The distinction between b values 10 and 100 was insignificant and the diagnostic value of images at b value 800 was low.

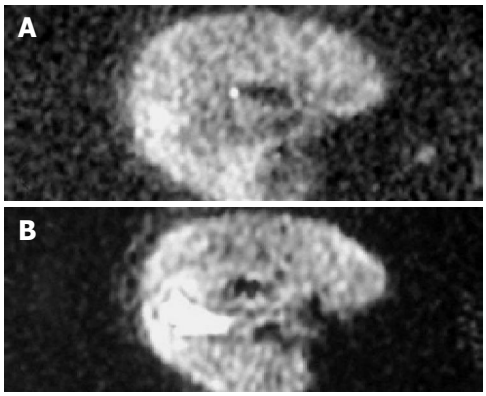

Figure 2 *b* value, the thickness and the NEX of image (**A**) were 300, 2 mm and 8 respectively while those of image (**B**) were 100, 2 mm and 1 respectively. The quality and SNR of the images were poorer than that of Figure 3.

When TR value was 4 000, 6 000 or 8 000, and other parameters were the same, ADC values of hepatic parenchyma

Table 2 DWI of normal rabbit liver with different *b* values (s/mm^2)

	b = 10	*b* = 50	*b* = 100	*b* = 300	*b* = 800	*F*	*P*
ADC[1]	3.23±0.41	2.92±0.43	2.58±0.41	1.73±0.37	0.93±0.56	292.87	<0.01
QI	12.74	12.07	11.80	7.87	3.98	156.1	<0.01
SNR	43.28	33.56	28.65	16.27	9.23	88.23	<0.01

[1](mean±SD)×10^{-3}mm^2/s.

were 2.48±0.52, 2.58±0.43 and 2.70±0.37 (F = 5.6, P<0.01) respectively, QI were 11.11, 11.80 and 10.83 (F = 3.15, P>0.05) respectively, and SNR were 26.61, 28.65 and 29.21 (F = 0.94, P>0.05) respectively, which indicates that QI and SNR did not change significantly. The distinction of ADC between TR 4 000 and 8 000 was significant (Tukey HSD, P<0.05) and that between TR 6 000 and 4 000 or 8 000 was not significant.

When the thickness was 2 or 5 mm and other parameters were the same, ADC values of hepatic parenchyma were 2.57±0.54 and 3.3±0.39 (t = -16.73, P<0.01) correspondingly, QI were 11.80 and 10.90 (t = 3.04, P<0.01) correspondingly and SNR were 28.65 and 71.56 (t = -17.86, P<0.01) correspondingly. The mean ADC value of the hepatic parenchyma and SNR of images were a great deal bigger, when the thickness was 5 mm than when the thickness was 2 mm, but QIs of images were smaller, when the thickness was 5 mm than when the thickness was 2 mm (Figure 3).

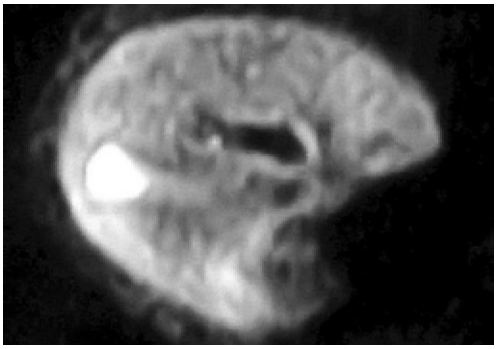

Figure 3 When *b* value was 100 and the thickness was 2 mm, SNR and the liver anatomy manifestation of the images were all good, while the artifact was low and the quality was high.

If rabbit liver was scanned with the cranium coil and the knee joint coil respectively while other parameters remained the same, QI of T1WI were 13.80 and 11.70 (t = 7.10, P<0.01) correspondingly and SNR of T1WI were 96.97 and 137.50 (t = -5.77, P<0.01) correspondingly while QI of T2WI were 11.23 and 9.71 (t = 3.97, P<0.01) correspondingly and SNR of T2WI were 36.41 and 43.63 (t = -4.02, P<0.01) correspondingly. SNR of the images was much bigger when the knee joint coil was used than when the cranium coil was used but QI of the images was smaller when the knee joint coil was used than when the cranium coil was used.

When FOV was 24 cm×24 cm, 20 cm×15 cm or 16 cm×12 cm while other parameters were the same, QI of T1WI were 12.87, 13.90 and 9.89 (F = 68.67, P<0.01) correspondingly and SNR of T1WI were 136.28, 96.97 and 52.03 (F = 85.81, P<0.01) respectively while QI of T2WI were 10.57, 11.23 and 7.45 (F = 69.46, P<0.01) correspondingly and SNR of T2WI were 47.86, 36.41 and 16.81 (F = 221.96, P<0.01) respectively. SNR of the images was the highest when FOV was 24 cm×24 cm and the smallest when FOV was 16 cm×12 cm and QI of the images was the highest when FOV was 20 cm×15 cm.

Based on 15 normal rabbit DWI with *b* value 100, TR 6 000 and thickness 2 mm, 13 images of the liver manifested average and high signals and the other two images of the liver did not manifest well due to the artifact. Eleven borders of the liver displayed well and the contrast between the liver and the neighboring organs was significant. The intrahepatic vessels of 10 cases manifested low signal and concentrated toward the first or the second porta hepatis. The intrahepatic bile ducts of four cases partly displayed high signal like the branches of a tree. All 15 cholecysts manifested high signal and part of them looked like "lamp bulbs". The VX-2 tumor manifested significantly high signal while surrounding hepatic parenchyma displayed low signal on DWI with a *b* value of 100, TR of 6 000 and a thickness of 2 mm. The distinction between VX-2 tumor and surrounding hepatic parenchyma was significant and the border of VX-2 tumor was clear (Figure 4).

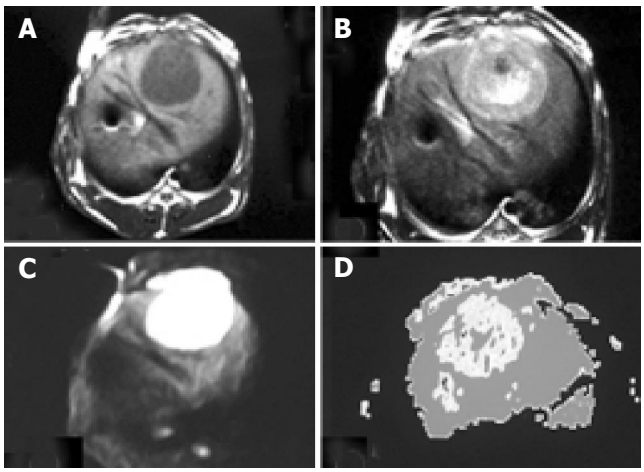

Figure 4 The VX-2 tumor manifests low signal on MR T1WI in image (A), while it displayed high signal on T2WI in image (B). The VX-2 tumor manifested significantly high signal while surrounding hepatic parenchyma displayed low signal on DWI in image (C) with b value 100, TR 6 000 and thickness 2 mm,the distinction between the VX-2 tumor and surrounding hepatic parenchyma was significant and the border of the VX-2 tumor was clear. The image (D) is the ADC map from VX-2 tumor DWI of the image (C).

DWI manifestation of rabbit liver

With *b* value, thickness, TR value, scanning coil and NEX were different, ADC value, the ability of liver anatomy manifestation or differentiation and SNR of rabbit liver on MR DWI were also different. In Figure 1, *b* values were respectively 10, 100, 300 and 800 s/mm^2 of the images (1), (2), (3) and (4). ADC value, SNR and the liver anatomy manifestation of the images became lower and lower with increasing *b* value. The distinction between *b* values 10 and 100 was insignificant and the diagnostic value of images at *b* value 800 was low. In Figure 2, *b* value, the thickness and the NEX of image (1) were 300, 2 mm and 8 respectively while those of image (2) were 100, 2 mm and 1 respectively. The quality and SNR of the images were poorer than that of Figure 3. In Figure 3, when *b* value was 100 and the thickness was 2 mm, SNR and the liver anatomy manifestation of the images were all good while the artifact was low and the quality was high. In Figure 4, the VX-2 tumor manifests low signal on MR T1WI in image (1), while it displayed high signal on T2WI in image (2). The VX-2 tumor manifested

significantly high signal while surrounding hepatic parenchyma displayed low signal on DWI in image (3) with *b* value 100, TR 6 000 and thickness 2 mm, the distinction between the VX-2 tumor and surrounding hepatic parenchyma was significant and the border of the VX-2 tumor was clear. The image (4) is the ADC map from VX-2 tumor DWI of the image (3).

DISCUSSION

Diffusion is caused by water molecular random motion, so-called "Brownian motion", and it is able to change the intensity of local magnetic field around hydrogen proton so that its phase position in the magnetic field is changed. When we added a powerful polar and quick switching gradient radiofrequent (RF) pulse besides routine RF pulse, we were able to amplify these phase changes so that we could detect water molecular diffusion motion, the so-called DWI. DWI was initially used to evaluate early ischemic stages of the brain and its value has been recognized in recent years. However, because of its poor image quality, DWI is rarely used in diagnosing and evaluating the lesions of the liver[24-28].

b value is the sensitivity of diffusion and it is the most important parameter of DWI scanning because changing it will directly lead to a change of the complemented gradient magnetic field and affect the ability of detecting water molecular diffusion. Ichikawa *et al*.[27,28], reported that high *b* value or *b* value deviation has an important influence on the quality of DWI and ADC value or DC value. When *b* value or its deviation is higher, ADC value would be stabler and could get closer to the DC value, which could better reflect water molecular diffusion motion, little affected by the microcirculation. When *b* value or its deviation is lower, ADC value will, to some degree, reflect the perfusion of the microcirculation while the ability of reflecting water molecular diffusion motion is worse than that of the former and the ADC value is also unstable. However, with increasing *b* value, gradient RF pulse will prolong, thus enlarging TE value, and the quality of images will be reduced[15,27,28]. Our results showed that ADC value, QI and SNR of the images would reduce with *b* value increase but, when *b* value was 100, QI of the images was basically the same as that when *b* value was 10 or 50 and SNR of the images was also better. Moreover, QI and SNR of the images were still high when *b* value was 300. Thus, we consider that at a *b* value of 100, QI and SNR of the images are good, together with a *b* value of 300, at which lesions are more sensitively detected as a good choice on DWI (Figures 1 and 3).

TR enlarging will raise the quality of the images because it prolongs the signal collecting time. But it leads to prolongation of the scanning time or reduction of the scanning coverage and it is not beneficial to control breathing. Our results indicated that the distinction of ADC between TR 4 000, 6 000 and 8 000 was significant ($P<0.01$) and that of QI or SNR was not significant. Because breathing has little influence on DWI after the rabbits are anesthetized generally and deeply, TR 6 000 is an appropriate choice and we may also choose a large NEX at the same time.

In our study, ADC value of hepatic parenchyma and SNR of images were significantly higher when the thickness was 5 mm than when it was 2 mm ($P<0.01$) and QI of the images were slightly higher when the thickness was 2 mm than when it was 5 mm ($P<0.01$). When the thickness is raised, SNR of images increases along with the increase of artifacts and decrease of the liver anatomy manifestations, which are not beneficial to the diagnosis of lesions. However, if we increase the collective information through enlarging NEX in order to compensate for the reduction due to the 2 mm thickness, we can obtain enough SNR and a good QI, especially for rabbit liver, which is small in volume andthe number of scans is limited and is not suitable for use in breath gating (Figures 2 and 3).

Both the knee joint coil and the cranium coil have applied reference in reported literature. Our results indicated that SNR of the knee joint coil group was higher than that of the cranium coil group ($P<0.01$), while QI of the knee joint coil group was lower than that of the cranium coil group ($P<0.01$). We found that the major reason for this was their clouding borders and artifacts because of small objective aperture of the knee joint coil, and effects of breathing movement. The cranium coil is a good choice for rabbit liver DWI because it is technically, the best.

As for FOV, it has a significant influence on the quality of DWI images. SNR of images increase with the increase in collective information as FOV enlarges, but QI do not increase continuously. This is because the liver anatomy manifestation decreases as the pixel enlarges and spatial resolution decreases due to the FOV increase. Small FOV (16 cm×12 cm) is not beneficial to diagnoses because of its small QI and SNR at the same time and we regard "20 cm×15 cm" as a more suitable FOV.

Due to the light weight, hair on body surface and quick breathing of rabbits, it was difficult to apply the technology of breath gating in rabbit liver DWI scanning. After rabbits were anesthetized by 3% soluble pentobarbitone injection into auricular vein, the breathing of rabbits was slow and stable; we acquired good images with SE-EPI series, the scan time was short, little affected by the respiratory movement. Our results indicated that the major reason for the artifact was the gas in the stomach and it was effective to use some precluding drug, fast the rabbits and use a stable and suitable posture to decrease the artifact.

In conclusion, the scanning techniques, including appropriate *b* value, thickness, coil, FOV, respiratory movement and control of stomach gas, are very important in DWI of rabbit liver and the overall quality of DWI with a *b* value (100 s/mm^2), thickness (2 mm), cranium coils and FOV (20 cm×15 cm) was considered the best in our study.

ACKNOWLEDGMENTS

We thank the staff of the Radiology Department and the Animal Department of the Second Xiangya Hospital for their help and support; particularly Miss. Ying-Si He.

REFERENCES

1 **Cai RL**, Meng W, Lu HY, Lin WY, Jiang F, Shen FM. Segregation analysis of hepatocellular carcinoma in a moderately high-incidence area of East China. *World J Gastroenterol* 2003; **9**: 2428-2432

2 **Braga L,** Guller U, Semelka RC. Modern hepatic imaging. *Surg Clin North Am* 2004; **84**: 375-400

3 **Choi BI.** The current status of imaging diagnosis of hepatocellular carcinoma. *Liver Transpl* 2004; **10**(2 Suppl 1): S20-S25

4 **Hussain SM,** Terkivatan T, Zondervan PE, Lanjouw E, de Rave S, Ijzermans JN, de Man RA. Focal nodular hyperplasia: findings at state-of-the-art MR imaging, US, CT, and pathologic analysis. *Radiographics* 2004; **24**: 3-17

5 **Koda M,** Matsunaga Y, Ueki M, Maeda Y, Mimura K, Okamoto K, Hosho K, Murawaki Y. Qualitative assessment of tumor vascularity in hepatocellular carcinoma by contrast-enhanced coded ultrasound: comparison with arterial phase of dynamic CT and conventional color/power Doppler ultrasound. *Eur Radiol* 2004; **14**: 1100-1108

6 **Vogl TJ,** Schwarz W, Blume S, Pietsch M, Shamsi K, Franz M, Lobeck H, Balzer T, del Tredici K, Neuhaus P, Felix R, Hammerstingl RM. Preoperative evaluation of malignant liver tumors: comparison of unenhanced and SPIO (Resovist)-enhanced MR imaging with biphasic CTAP and intraoperative US. *Eur Radiol* 2003; **13**: 262-272

7 **Vilana R,** Llovet JM, Bianchi L, Sanchez M, Pages M, Sala M, Gilabert R, Nicolau C, Garcia A, Ayuso C, Bruix J, Bru C. Contrast-enhanced power doppler sonography and helical computed tomography for assessment of vascularity of small hepatocellular carcinomas before and after percutaneous ablation. *J Clin Ultrasound* 2003; **31**: 119-128

8 **Minami Y,** Kudo M, Kawasaki T, Kitano M, Chung H, Maekawa K, Shiozaki H. Transcatheter arterial chemoembolization of hepatocellular carcinoma: usefulness of coded phase-inversion harmonic sonography. *Am J Roentgenol* 2003; **180**: 703-708

9 **Ward J,** Robinson PJ. How to detect hepatocellular carcinoma in cirrhosis. *Eur Radiol* 2002; **12**: 2258-2272

10 **Nijsen JF,** Seppenwoolde JH, Havenith T, Bos C, Bakker CJ, van het Schip AD. Liver tumors: MR imaging of radioactive holmium microspheres-phantom and rabbit study. *Radiology* 2004; **231**: 491-499

11 **Lee JW,** Moon WK, Weinmann HJ, Kim SJ, Kim JH, Park SH, Kim TJ, Yoon CJ, Kim YH, Cho EY, Ha SW, Kang WS, Chang KH. Contrast-enhanced MR imaging of postoperative scars and VX2 carcinoma in rabbits: comparison of macromolecular contrast agent and gadopentetate dimeglumine. *Radiology* 2003; **229**: 132-139

12 **Forsberg F,** Piccoli CW, Liu JB, Rawool NM, Merton DA, Mitchell DG, Goldberg BB. Hepatic tumor detection: MR imaging and conventional US versus pulse-inversion harmonic US of NC100100 during its reticuloendothelial system-specific phase. *Radiology* 2002; **222**: 824-829

13 **Sayegh Y,** Pochon S, Vallee JP, Becker M, Lazeyras F, Tournier H, Hyacinthe R, Fouillet X, Terrier F. Detection of experimental hepatic tumors using long circulating superparamagnetic particles. *Invest Radiol* 2001; **36**: 15-21

14 **Geschwind JF,** Artemov D, Abraham S, Omdal D, Huncharek MS, McGee C, Arepally A, Lambert D, Venbrux AC, Lund GB. Chemoembolization of liver tumor in a rabbit model: assessment of tumor cell death with diffusion-weighted MR imaging and histologic analysis. *J Vasc Interv Radiol* 2000; **11**: 1245-1255

15 **Kuszyk BS,** Boitnott JK, Choti MA, Bluemke DA, Sheth S, Magee CA, Horton KM, Eng J, Fishman EK. Local tumor recurrence following hepatic cryoablation: radiologic-histopathologic correlation in a rabbit model. *Radiology* 2000; **217**: 477-486

16 **Miao Y,** Ni Y, Mulier S, Yu J, De Wever I, Penninckx F, Baert AL, Marchal G. Treatment of VX2 liver tumor in rabbits with "wet" electrode mediated radio-frequency ablation. *Eur Radiol* 2000; **10**: 188-194

17 **Sun XJ,** Quan XY, Liang W, Wen ZB, Zeng S, Huang FH, Tang M. Quantitative study of diffusion weighted imaging on magnetic resonance imaging in focal hepatic lesions less than 3 cm. *Zhonghua Zhongliu Zazhi* 2004; **26**: 165-167

18 **Cheryauka AB,** Lee JN, Samsonov AA, Defrise M, Gullberg GT. MRI diffusion tensor reconstruction with PROPELLER data acquisition. *Magn Reson Imaging* 2004; **22**: 139-148

19 **Chow LC,** Bammer R, Moseley ME, Sommer FG. Single breath-hold diffusion-weighted imaging of the abdomen. *J Magn Reson Imaging* 2003; **18**: 377-382

20 **Kamel IR,** Bluemke DA, Ramsey D, Abusedera M, Torbenson M, Eng J, Szarf G, Geschwind JF. Role of diffusion-weighted imaging in estimating tumor necrosis after chemoembolization of hepatocellular carcinoma. *Am J Roentgenol* 2003; **181**: 708-710

21 **Boulanger Y,** Amara M, Lepanto L, Beaudoin G, Nguyen BN, Allaire G, Poliquin M, Nicolet V. Diffusion-weighted MR imaging of the liver of hepatitis C patients. *NMR Biomed* 2003; **16**: 132-136

22 **Taouli B,** Vilgrain V, Dumont E, Daire JL, Fan B, Menu Y. Evaluation of liver diffusion isotropy and characterization of focal hepatic lesions with two single-shot echo-planar MR imaging sequences: prospective study in 66 patients. *Radiology* 2003; **226**: 71-78

23 **Inoha S,** Inamura T, Nakamizo A, Ikezaki K, Amano T, Fukui M. Magnetic resonance imaging in cases with encephalopathy secondary to immunosuppressive agents. *J Clin Neurosci* 2002; **9**: 305-307

24 **Murtz P,** Flacke S, Traber F, van den Brink JS, Gieseke J, Schild HH. Abdomen: diffusion-weighted MR imaging with pulse-triggered single-shot sequences. *Radiology* 2002; **224**: 258-264

25 **Moteki T,** Horikoshi H, Oya N, Aoki J, Endo K. Evaluation of hepatic lesions and hepatic parenchyma using diffusion-weighted reordered turboFLASH magnetic resonance images. *J Magn Reson Imaging* 2002; **15**: 564-572

26 **Chan JH,** Tsui EY, Luk SH, Fung AS, Yuen MK, Szeto ML, Cheung YK, Wong KP. Diffusion-weighted MR imaging of the liver: distinguishing hepatic abscess from cystic or necrotic tumor. *Abdom Imaging* 2001; **26**: 161-165

27 **Ichikawa T,** Haradome H, Hachiya J, Nitatori T, Araki T. Diffusion-weighted MR imaging with a single-shot echoplanar sequence: detection and characterization of focal hepatic lesions. *AJR Am J Roentgenol* 1998; **170**: 397-402

28 **Ichikawa T,** Haradome H, Hachiya J, Nitatori T, Araki T. Diffusion-weighted MR imaging with single-shot echo-planar imaging in the upper abdomen: preliminary clinical experience in 61 patients. *Abdom Imaging* 1999; **24**: 456-461

Science Editor Zhu LH and Guo SY **Language Editor** Elsevier HK